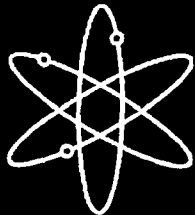




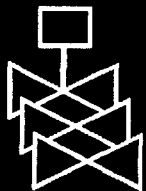
Posttest Analysis of the Steel Containment Vessel Model



Sandia National Laboratories



U.S. Nuclear Regulatory Commission
Office of Nuclear Regulatory Research
Washington, DC 20555-0001



AVAILABILITY NOTICE

Availability of Reference Materials Cited in NRC Publications

NRC publications in the NUREG series, NRC regulations, and *Title 10, Energy, of the Code of Federal Regulations*, may be purchased from one of the following sources:

1. The Superintendent of Documents
U.S. Government Printing Office
P.O. Box 37082
Washington, DC 20402-9328
<http://www.access.gpo.gov/su_docs>
202-512-1800
2. The National Technical Information Service
Springfield, VA 22161-0002
<<http://www.ntis.gov>>
1-800-553-6847 or locally 703-605-6000

The NUREG series comprises (1) brochures (NUREG/BR-XXXX), (2) proceedings of conferences (NUREG/CP-XXXX), (3) reports resulting from international agreements (NUREG/IA-XXXX), (4) technical and administrative reports and books [(NUREG-XXXX) or (NUREG/CR-XXXX)], and (5) compilations of legal decisions and orders of the Commission and Atomic and Safety Licensing Boards and of Office Directors' decisions under Section 2.206 of NRC's regulations (NUREG-XXXX).

A single copy of each NRC draft report for comment is available free, to the extent of supply, upon written request as follows:

Address: Office of the Chief Information Officer
Reproduction and Distribution
Services Section
U.S. Nuclear Regulatory Commission
Washington, DC 20555-0001

E-mail: <DISTRIBUTION@nrc.gov>
Facsimile: 301-415-2289

A portion of NRC regulatory and technical information is available at NRC's World Wide Web site:

<<http://www.nrc.gov>>

After January 1, 2000, the public may electronically access NUREG-series publications and other NRC records in NRC's Agencywide Document Access and Management System (ADAMS), through the Public Electronic Reading Room (PERR), link <<http://www.nrc.gov/NRC/ADAMS/index.html>>.

Publicly released documents include, to name a few, NUREG-series reports; *Federal Register* notices; applicant, licensee, and vendor documents and correspondence; NRC correspondence and internal memoranda; bulletins and information notices; inspection and investigation reports; licensee event reports; and Commission papers and their attachments.

Documents available from public and special technical libraries include all open literature items, such as books, journal articles, and transactions, *Federal Register* notices, Federal and State legislation, and congressional reports. Such documents as theses, dissertations, foreign reports and translations, and non-NRC conference proceedings may be purchased from their sponsoring organization.

Copies of industry codes and standards used in a substantive manner in the NRC regulatory process are maintained at the NRC Library, Two White Flint North, 11545 Rockville Pike, Rockville, MD 20852-2738. These standards are available in the library for reference use by the public. Codes and standards are usually copyrighted and may be purchased from the originating organization or, if they are American National Standards, from—

American National Standards Institute
11 West 42nd Street
New York, NY 10036-8002
<<http://www.ansi.org>>
212-642-4900

DISCLAIMER

This report was prepared as an account of work sponsored by an agency of the United States Government. Neither the United States Government nor any agency thereof, nor any of their employees, makes any warranty, expressed or implied, or assumes

any legal liability or responsibility for any third party's use, or the results of such use, of any information, apparatus, product, or process disclosed in this report, or represents that its use by such third party would not infringe privately owned rights.

NUREG/CR-6649
SAND 99-2954

Posttest Analysis of the Steel Containment Vessel Model

Manuscript Completed: February 1999
Date Published: February 2000

Prepared by
J. S. Ludwigsen, V. K. Luk, M. F. Hessheimer

Sandia National Laboratories
Albuquerque, NM 87185

J. F. Costello, NRC Project Manager

Prepared for
Division of Engineering Technology
Office of Nuclear Regulatory Research
U.S. Nuclear Regulatory Commission
Washington, DC 20555-0001
NRC Job Code A1401



**NUREG/CR-6649 has been reproduced
from the best available copy.**

Abstract

The Nuclear Power Engineering Corporation (NUPEC) of Japan and the US Nuclear Regulatory Commission (NRC), Office of Nuclear Regulatory Research, are co-sponsoring and jointly funding a Cooperative Containment Research Program* at Sandia National Laboratories (SNL), Albuquerque, NM, USA. As a part of this program, a steel containment vessel (SCV) model and contact structure assembly was tested to failure with overpressurization at SNL on December 11–12, 1996. The SCV model is a mixed-scale model (1:10 in geometry and 1:4 in shell thickness) of a steel containment for an improved Mark-II Boiling Water Reactor (BWR) plant in Japan. The contact structure, which is a thick, bell-shaped steel shell separated at a nominally uniform distance from the SCV model, provides a simplified representation of some features of the concrete reactor shield building in the actual plant. The objective of the internal pressurization test is to provide measurement data of the structural response of the SCV model up to its failure in order to validate analytical modeling, to find its pressure capacity, and to observe the failure mode and mechanisms.

Prior to the high pressure test, a pretest analysis of the SCV model was performed to predict the model response to loads beyond the design basis conditions. The posttest analysis effort started with a detailed comparison of the pretest analysis results to the high pressure test data. This comparison identified the areas where the pretest analysis results did not match well with the measured data. Based on these findings, the posttest analyses were undertaken to investigate whether modeling changes, such as the more accurate material models, and local structural and material details around the two tears in the SCV model developed during the high pressure test, could improve the analytical predictions.

This report documents the comparison of the pretest predictions and the posttest simulations of the structural response of the SCV model to the high pressure test data. The lessons learned from the analysis effort are also summarized.

* The Nuclear Power Engineering Corporation and the U.S. Nuclear Regulatory Commission jointly sponsor this work at Sandia National Laboratories. The work of the Nuclear Power Engineering Corporation is performed under the auspices of the Ministry of International Trade and Industry, Japan. Sandia is a multiprogram laboratory operated by Sandia Corporation, a Lockheed Martin Company, for the U.S. Department of Energy under Contract Number DE-AC04-94AL85000.

Contents

Abstract.....	iii
Executive Summary.....	vii
Acknowledgments.....	ix
Acronyms.....	xi
1. INTRODUCTION.....	1-1
2. MATERIAL AND FINITE ELEMENT ANALYSIS MODELS.....	2-1
2.1 Material Modeling.....	2-1
2.1.1 SGV480 and SPV490 Material Models.....	2-1
2.1.2 Finite Element Analysis Models.....	2-3
3. GLOBAL ANALYSIS.....	3-1
3.1 Comparison of Pretest Predictions to Test Data.....	3-1
3.2 Posttest Analyses.....	3-1
4. LOCAL ANALYSES.....	4-1
4.1 Strength Reduction for SPV490 Heat Affected Zone (HAZ).....	4-1
4.2 Equipment Hatch Analysis.....	4-3
4.3 Middle Stiffening Ring Analysis.....	4-6
4.4 Failure Considerations of SCV Model.....	4-8
5. SUMMARY.....	5-1
6. REFERENCES.....	6-1

Figures

1.1 Steel containment vessel (SCV) model elevation.....	1-2
2.1 Coupon test data and the stress-strain curves used in the pretest analysis for 8.5 mm SGV480 steel alloy.....	2-2
2.2 Coupon test data and the stress-strain curve used in the posttest analysis for 9 mm SPV490 steel alloy ...	2-2
2.3 Global three-dimensional finite element representation of steel containment vessel (SCV) model.....	2-3
2.4 Local three-dimensional finite element model of equipment hatch with SPV490 heat affected zone (HAZ) elements shown in black.....	2-5
2.5 The finite element model used to investigate the small tear.....	2-5
3.1 Radial deflections of the steel containment vessel (SCV) model (magnified by a factor of ten) at 4.5 MPa versus model elevation.....	3-2

3.2	Interior hoop strains at upper conical shell section at Round Robin Standard Output Location #24	3-2
3.3	Exterior hoop strains at upper conical shell section	3-3
3.4	Hoop strains at 270° meridian and 4.5 MPa versus the steel containment vessel (SCV) model elevation ..	3-4
4.1	True stress versus true strain relationship for 9 mm SPV490 base metal and heat affected zone (HAZ) ...	4-2
4.2	Correlation of Rockwell B hardness number to ultimate strength of SPV490 steel	4-3
4.3	An instrumentation layout on the interior of the equipment hatch area	4-4
4.4	Schematic of the equipment hatch area from inside the SCV model	4-4
4.5	Interior view of equipment hatch area with an arrow pointing to large tear	4-5
4.6	Strain contours around the equipment hatch from the pretest analysis	4-5
4.7	Strain contours around the equipment hatch from the posttest analysis	4-6
4.8	A small tear inside a weld relief opening at the middle stiffening ring	4-7
4.9	Close-up view of the weld relief opening at the middle stiffening ring from a local three-dimensional finite element model	4-7
4.10	A contour plot of the equivalent plastic strains on the inside surface of the steel containment vessel (SCV) model at a pressure of 4.7 MPa	4-8
4.11	Outward radial displacement of steel containment vessel (SCV) wall at small tear location without the presence of contact structure	4-9
4.12	A contour plot of equivalent plastic strains on the steel containment vessel (SCV) wall adjacent to the weld relief opening at a pressure of 4.0 MPa	4-9

Executive Summary

For the past twenty years, Sandia National Laboratories (SNL) tested and analyzed numerous scale models of containment vessels that had been pressurized to failure as a part of the Containment Integrity Programs sponsored by the US Nuclear Regulatory Commission (NRC). The overall objective of the programs was to investigate the adequacy of analytical methods used to predict the performance of light water reactor (LWR) containment vessels subject to loads beyond the design basis. Five scale models of steel containment vessels and a reinforced concrete containment model were tested.

Starting in 1991, SNL has been working on a Cooperative Containment Research Program for LWR containments under the joint sponsorship of the Nuclear Power Engineering Corporation (NUPEC) of Tokyo, Japan, and the NRC. This program involves the overpressurization tests of two scale models: a steel containment vessel (SCV) model of an improved Mark-II boiling water reactor (BWR) containment vessel and a prestressed concrete containment vessel (PCCV) model. This report discusses the posttest analyses of the internal pressurization test on the SCV model. The SCV model used a mixed-scale design with 1:10 for the geometry scale and 1:4 for the thickness scale. The objective of the test was to collect measurement data of the structural response of the SCV model up to its failure to validate analytical modeling, to find its pressure capacity, and to observe the failure model and mechanisms.

The test assembly includes a bell-shaped steel contact structure (CS) at a nominally uniform distance from the SCV model. The uniform gap between these two structures permits the SCV model to undergo deformation well beyond the elastic range prior to making contact with the CS. The presence of the CS, a much simplified representation of a concrete shield building in a physical plant, facilitated a study of the SCV model behavior after it made contact with the CS. The SCV/CS structural assembly provided specific features of the interaction to be investigated, including closure of gap, progression of contact, and load sharing between the SCV model and the CS.

Prior to the SCV high pressure test that was conducted at SNL on December 11–12, 1996, a pretest analysis of the SCV model was performed to predict the model response to loads beyond the design basis conditions. The posttest analysis effort started with a detailed comparison of the pretest analysis results to the high pressure test data. This comparison identified the areas where the pretest analysis results did not match well with the measured data. Based on these findings, the posttest analyses were undertaken to improve the analytical predictions by making a few modeling changes, such as the more accurate material models, and local structural and material details around the two tears in the SCV model developed during the high pressure test.

The posttest analysis effort focused on using more accurate material models for SGV480 and SPV490 steel alloys in the SCV model, especially around the yield limit of materials. The posttest inspection of the SCV model revealed that there were two tears developed in the SCV model during the high pressure test. A large tear, about 190 mm long, was found along the edge of the equipment hatch reinforcement plate. An approximate material model for the SPV490 heat affected zone, which was not identified prior to the high pressure test, was implemented in the posttest analysis to simulate the local high strain concentrations responsible for initiating and propagating this tear. Another small tear, approximately 55 mm long, was found next to a meridional weld inside a semi-circular weld relief opening at the middle stiffening ring. A local three-dimensional finite element model, which incorporated the local structural details around this area, was developed to investigate the cause of the occurrence of the small tear there. The gap size between the SCV model and the CS was also increased from 18 mm to 22 mm to provide a better representation of the as-built configuration. After the structural details characteristic of the local configuration were incorporated in the finite element models, it has been demonstrated that the posttest analysis can produce results of the deformation behavior of the SCV model very similar to the test data.

This report documents the comparison of the pretest predictions and the posttest simulations of the structural response of the SCV model to the high pressure test data. The lessons learned about the use of finite element calculations from the analysis effort are also summarized.

Acknowledgments

The posttest analyses would not have been completed without the support and cooperation of the project members who provided the systematic tabulation of high pressure test data and performed the posttest metallurgical evaluation of the SCV model. Their effort is deeply appreciated.

The authors acknowledge the guidance, support, and encouragement from Dr. Hideo Ogasawara, Director and General Manager, Systems Safety Department, Nuclear Power Engineering Corporation (NUPEC) of Tokyo, Japan. The authors are also indebted to Dr. James F. Costello, Senior Structural Engineer, Engineering Research Applications Branch, Division of Engineering Technology, Nuclear Regulatory Commission, for his continuous technical guidance and encouragement.

Acronyms

BWR	boiling water reactor
CS	contact structure
HAZ	heat affected zone
LWR	light water reactor
NRC	Nuclear Regulatory Commission
NUPEC	Nuclear Power Engineering Corporation
PCCV	prestressed concrete containment vessel
SCV	steel containment vessel
SNL	Sandia National Laboratories

1. INTRODUCTION

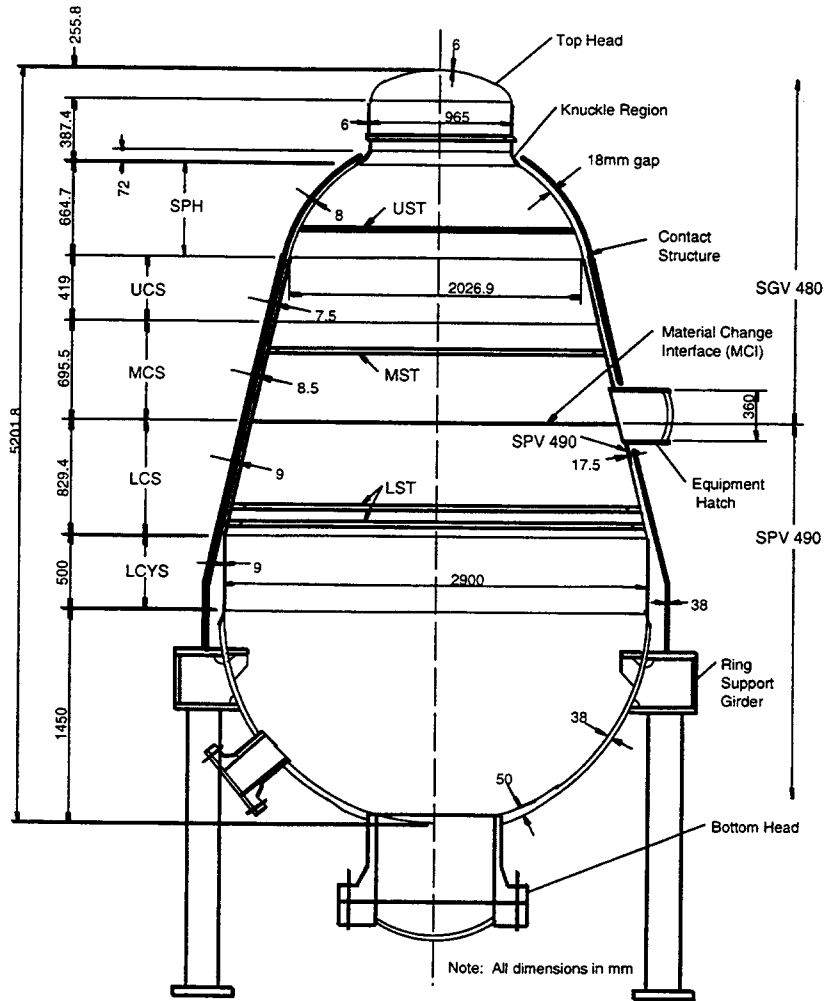
The Nuclear Power Engineering Corporation (NUPEC) of Japan and the US Nuclear Regulatory Commission (NRC) are co-sponsoring a Cooperative Containment Research Program at Sandia National Laboratories (SNL), Albuquerque, NM, USA. The purpose of the program is to investigate the response of representative models of nuclear containment structures to pressure loads beyond the design basis accident. This investigation includes conducting pneumatic overpressurization tests of scale models to failure and an analysis program to compare analytical predictions to measured behavior. As a part of the research program, a scaled steel containment vessel (SCV) test model of an improved Mark-II Boiling Water Reactor (BWR) containment was pressurized to failure during a high pressure test conducted December 11–12, 1996 at SNL.

This report is one of a series of reports that discusses the testing of the SCV model to failure. Prior to the SCV high pressure test, a pretest analysis of the SCV model was performed to predict the model response to loads beyond the design basis conditions (Porter et al., 1998). The SCV Round Robin Pretest Analysis Report (Luk and Klamerus, 1998) summarizes the pretest predictions from several organizations around the world that were invited to participate in the analysis effort. A Round Robin Posttest Analysis Report (Luk and Klamerus, 1999) summarizes the posttest analyses from the same organizations. Both of the Round Robin reports concentrated on providing the predicted SCV model behavior at 43 standard output locations. The Round Robin posttest report added 10 additional output locations to the 43 for comparisons between analysis results and test data. In addition, an SCV Test Report (Luk et al., 1999) provides a detailed account of the test operation and includes the data from the instrumentation installed in the model.

This report describes the posttest structural analyses of the SCV model. A sketch of the SCV model showing the inner containment structure and the outer contact structure is shown in Figure 1.1. The model was a nominal 1:10 scale in the overall dimensions with the material thickness scaled at a 1:4 ratio. The mixed scaling was used to keep the plate thickness of the SCV model large enough to manufacture and weld using the same methods as those used on the actual containments. The nominal scaled design pressure was 0.78 MPa. The contact structure was installed over the SCV model to simulate the effects of contact with a relatively rigid structure. Reinforced concrete shield buildings surround the actual containment vessels, and contact can be expected in some severe accident scenarios.

The posttest analysis effort started with a detailed comparison of the pretest analysis results to the high pressure test data. This comparison identified the areas where the pretest analysis results did not match well with the measured data. Based on these findings, the posttest analyses were undertaken to investigate whether modeling changes could improve the predictions.

The material models were revised for the two steel alloys, SGV480 and SPV490, in the SCV model, and they were used in global and local finite element models for the posttest calculations. These modeling methodologies and procedures are described in Chapter 2. The predictions of global response, with emphasis on determining the load level required to cause global yielding at the free-field locations away from structural discontinuities such as the equipment hatch, are evaluated in Chapter 3. The predictions of local response, with emphasis on the locations where the two tears were observed, are treated in Chapter 4. Chapter 5 summarizes the lessons learned through the pretest and posttest analyses.



Nomenclature:

Location Designation	Description
THD	top head
KNU	knuckle
SPH	spherical shell
UST	upper stiffener
UCS	upper conical shell
MST	middle stiffener
MCS	middle conical shell
MCI	material change interface
LCS	lower conical shell
LST	lower stiffeners
LCYS	lower cylindrical shell

Figure 1.1 Steel containment vessel (SCV) model elevation

2. MATERIAL AND FINITE ELEMENT ANALYSIS MODELS

2.1 Material Modeling

Uniaxial tensile tests were performed on the coupons of the virgin SGV480 and SPV490 steel plates with various thicknesses (Porter et al., 1998). Material models, based on the tensile test data, were used in the pretest analyses. The posttest analysis effort focused on evaluating these material models to identify possible remedies to improve the discrepancies between the pretest predictions and the measured high pressure test data.

2.1.1 SGV480 and SPV490 Material Models

The measured data from the high pressure test of the steel containment vessel (SCV) model showed that the majority of the structure experienced plastic strains of generally less than 2 percent. The pretest analyses concentrated more on the stress-strain relationships in the high-strain regions (over 20 percent) so that the high strains associated with the model failure could be accurately tied to the pressure load on the structure. The emphasis on the mechanical properties of higher strains was done to meet one of the major goals of the pretest analysis, i.e., to predict the failure pressure.

To accurately represent the material properties of a high stress-strain relationship in the pretest analyses, a theoretical hardening curve, such as a power law or an inverse hyperbolic sine law, was used to fit the true stress versus true strain data. This method provides good accuracy at the higher-strain regimes, and more importantly for the pretest analyses, it provided some confidence based on experience with other steel models in the stress-strain relationship at strains past the ultimate load in the coupon test data. Unfortunately, the analytical material model had some error at the lower strains. These analytical models tended to overestimate the strength of the materials at low strains.

In hindsight, this emphasis on the material behavior of high strains was not as important as was first thought for two reasons. First, as mentioned previously, the major portion of the SCV model experienced strains below 2 percent. Second, a finite element mesh of a large structure will not include many of the structural details that can lead to localize high-strain conditions in small areas. The areas that do

exhibit strains beyond the maximum stress levels are usually associated with a structure detail, such as a weld or a subtle change in geometry, which is smaller than the average element size. This means that the increased strain concentrations associated with these local features will not be predicted or will be averaged within the element formulation. A more detailed finite element model would be required to lead to predictions of over 20 percent strain levels.

Figure 2.1 shows the coupon test data and the stress-strain curve used in the pretest analysis for the 8.5 mm SGV480 steel alloy. The differences in the pretest curve and the coupon test data at levels below 5 percent strain are obvious in this figure. At higher-strain regimes, the match between the measured material data and the analytical material model is very good.

For the posttest analysis, a much simpler approach was used to model the material behavior. The plastic behavior of the material was modeled by simply using the lower envelope of the plotted true stress versus true strain from the coupon tests. The elastic portion of the stress-strain curves assumed a standard value for the Young's modulus. The choice of using the lower envelope of the stress-strain curves was meant to be conservative with regard to the material strengths. Even with the use of the lower envelope, factors such as the residual stress (Pfeiffer and Kulak, 1988) in the as-built configuration of the SCV model and the variations in material properties throughout the plate are not reflected in the material model. As documented in Pfeiffer and Kulak (1988), the residual stress does not play a dominant role in the behavior of structures in the plastic domain. The SGV480 coupon tests did not show significant differences between the rolled and transverse directions; therefore the same material model was used for the two directions.

In Figure 2.2, the coupon test data for the 9 mm SPV490 steel alloy and the assumed stress-strain curve used in the posttest analysis are shown. There is a considerable difference between the material properties in rolled and transverse directions. Because the orientation of the SPV490 plates in the SCV model placed during the manufacturing process was unknown, the lower envelope of the two curves was used for both directions in the analytical model.

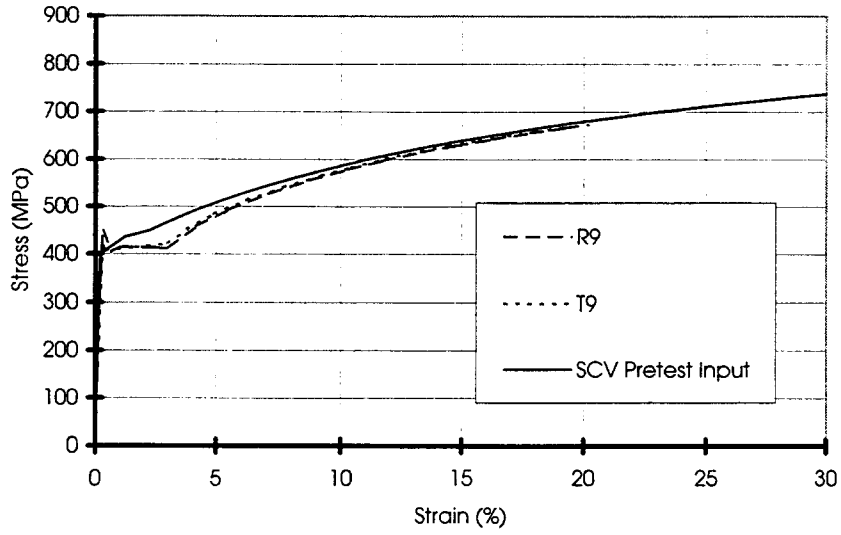


Figure 2.1 Coupon test data and the stress-strain curves used in the pretest analysis for 8.5 mm SGV480 steel alloy

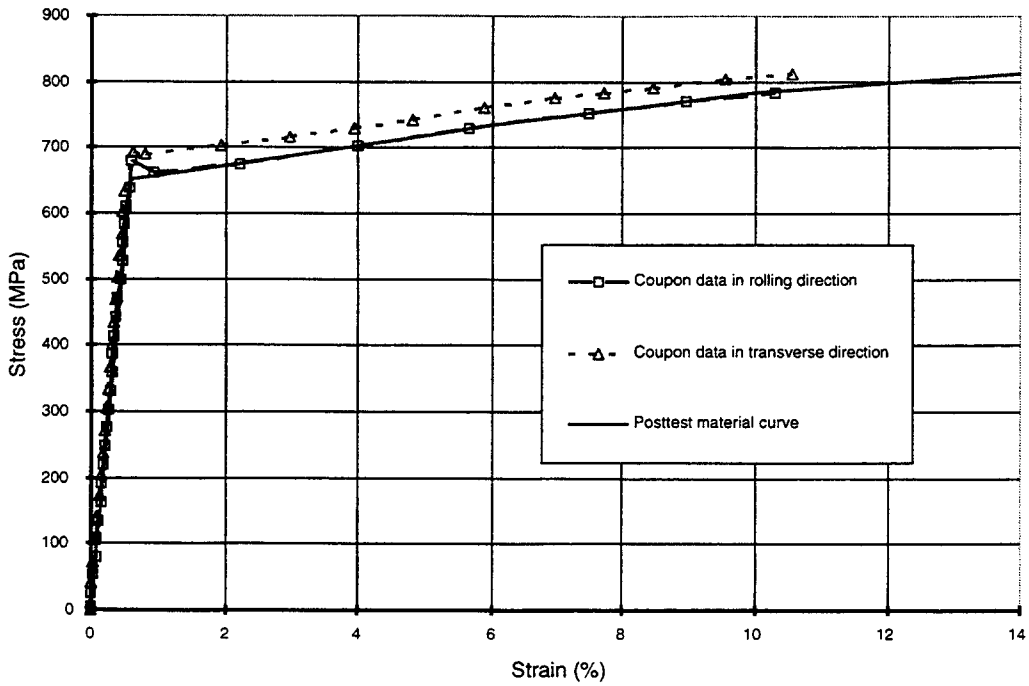


Figure 2.2 Coupon test data and the stress-strain curve used in the posttest analysis for 9 mm SPV490 steel alloy

2.1.2 Finite Element Analysis Models

2.1.2.1 Global Analysis Model

The global three-dimensional finite element model of the SCV model and contact structure is shown in Figure 2.3. The ABAQUS finite element code version 5.6 was used to analyze this global model for the posttest analysis effort (ABAQUS, 1995). The half-symmetry model used approximately 4,800 four-node reduced integration shell elements with finite membrane strain capability (ABAQUS S4R elements). The only non-axisymmetric detail included in this model is the equipment hatch. Symmetric boundary conditions were imposed on all nodes lying in the vertical (x,y) plane passing through the centerline of the equipment hatch, and vertical displacements were constrained at the support locations on the underside of the ring support girder. The loading consisted of the internal pressure, and the analysis was executed until a preset limit of 5 MPa internal pressure was reached. This preset pressure was greater than the failure pressure of 4.66 MPa during the high pressure test. The nominal gap between the SCV model and the contact structure was increased from the nominal 18 mm that was specified in the design and used in the pretest analysis to 22 mm to better reflect the as-built configuration.

Many of the features used in the pretest global analyses were retained for the posttest analyses. The mod-

eling specifics of the contact between the SCV model and the contact structure were not changed. In both the pretest and the posttest models, a small sliding formulation was used because the relative sliding of the SCV model and the contact structure was assumed to be small. The friction coefficient, $\mu=0.2$, was used for both as well.

The thickened equipment hatch reinforcement plate was constructed in such a way that it is flush with the inside surface of the SCV model. The thickness eccentricity poses a problem when using the shell elements in the ABAQUS code because there are no means of explicitly modeling a shell with uneven material distribution about a reference line. A simple elastic test case performed in the pretest analysis showed that using the *SHELL SECTION COMPOSITE option in the ABAQUS code is an accurate way of implicitly modeling the eccentricity at the equipment hatch reinforcement plate (ABAQUS, 1995). The equipment hatch reinforcement plate was modeled as a composite shell with three layers. The eccentricity was introduced by making the middle layer the same thickness as the adjacent material and then placing two shells with the same thickness on either side. The middle and outside layers were given the modulus of elasticity for the equipment hatch reinforcement plate measured from the coupon tensile tests, while the inner composite layer was

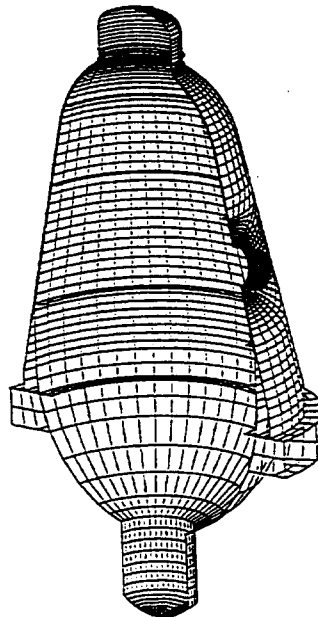


Figure 2.3 Global three-dimensional finite element representation of steel containment vessel (SCV) model

given a very low dummy modulus. This formulation makes the stiffness of the inner layer of the composite shell negligible with respect to the outer layer causing an effective eccentricity in the connection of the two materials.

Because of the eccentricity at the equipment hatch reinforcement plate, the measured gap between this plate and the contact structure was reduced considerably to approximately 13 mm. The eccentricity formulation described above does not account for the smaller gap because the contact algorithm uses the centerlines of both the composite shells in the equipment hatch reinforcement plate and the regular shells in the contact structure as the references. Therefore, the gap between the equipment hatch reinforcement plate and the contact structure in the global finite element model is 22 mm.

The gap between the SCV model and the contact structure near the knuckle region was also increased radially by 4 mm. Because of the slope of the model wall in this location, the gap also grew in the vertical direction. The resulting total gap was then larger than the as-built dimension. The increased gap dimension allowed more vertical deformation to take place in the model.

2.1.2.2 Local Analysis Models

The posttest metallurgical evaluation identified a local heat affected zone (HAZ) of the SPV490 plate along the weld seam of the equipment hatch reinforcement plate (Van Den Avyle and Eckelmeyer, 1999). This locally weakened area experienced a strong local necking deformation resulting in the development of the large tear. An approximate material model for the SPV490 HAZ with reduced strength was developed, and its details are described in Chapter 4. Figure 2.4 shows a local three-dimensional model of the equipment hatch using this approximate material model to simulate the HAZ that was represented by a strip of elements labeled in black.

A local three-dimensional model was developed of the middle stiffening ring, including the weld relief opening where the small tear occurred. Figure 2.5 shows the finite element model to investigate the occurrence and propagation of this tear. The large size of the finite element model was chosen so that the membrane forces in the SCV model wall around the small tear would be modeled accurately. The finite element code JAS3D (Blanford, 1998) was used for this analysis, although any general purpose finite element code could have been used for this problem.

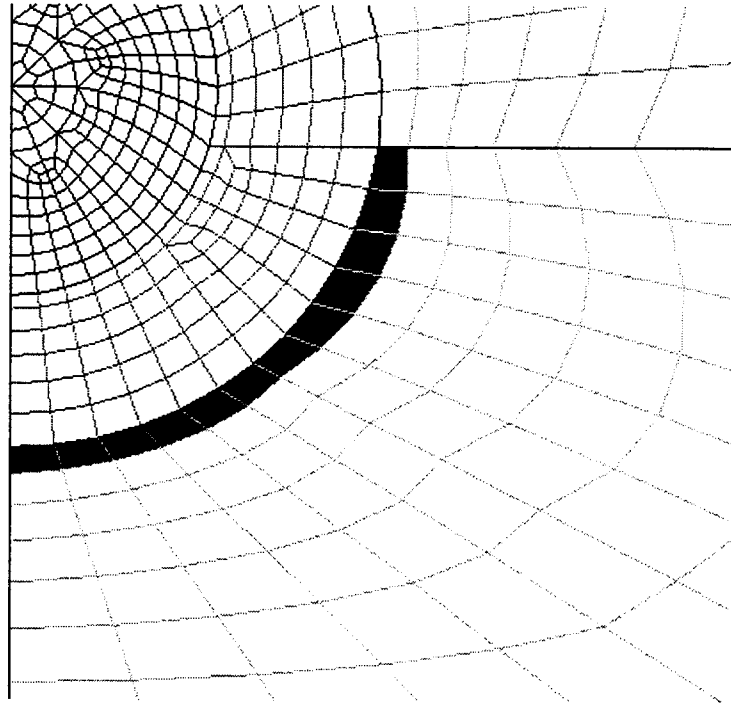


Figure 2.4 Local three-dimensional finite element model of equipment hatch with SPV490 heat affected zone (HAZ) elements shown in black

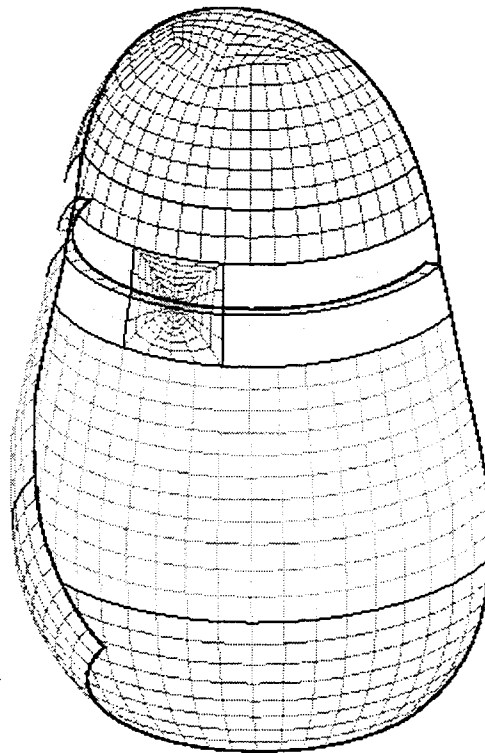


Figure 2.5 The finite element model used to investigate the small tear

3. GLOBAL ANALYSIS

The posttest analysis efforts started with an investigation into the global response of the steel containment vessel (SCV) model at a free-field location far away from the local structural complexities such as the equipment hatch. The investigative procedure began with a comparison of the pretest predictions at the chosen free-field location on the SCV model to the data from the high pressure test. After the discrepancies between these two sets of results were identified, different remedies were developed and evaluated to resolve these disagreements. The post-test analysis results were compared to the pretest predictions and the test data to demonstrate the improvements in the modeling procedures and the analytical capabilities of finite element codes.

3.1 Comparison of Pretest Predictions to Test Data

In general, the global response of the SCV model behaves in an axisymmetric manner in the free-field areas away from the equipment hatch. For this reason, the first measure of the pretest predictions was to compare the global responses where the finite element formulation should have been able to accurately capture the global behavior. Figure 3.1 shows the radial deflections of the SCV model at a pressure of 4.5 MPa along the 270° meridian, which is at the opposite side of the equipment hatch. The pretest analysis results and the measured data are shown on the initial contour of the SCV model with a magnification factor of 10 applied to the displacements. Some of the data points in the high pressure test data are interpolated between two measured locations. Therefore the difference between the measured and analysis results at elevations of 1,500 mm and 2,200 mm are not as severe as the figure indicates.

Figure 3.1 shows that the pretest predictions tended to underestimate the radial displacements at the pressure of 4.5 MPa. This observation is consistent with the free-field hoop strain gage data where the pretest analysis consistently overestimated the SCV model stiffness. A typical free-field behavior is represented by the hoop strain response at the upper conical shell section, such as the Round Robin Standard Output Location #24 (Luk and Klamerus, 1998), where a rosette strain gage, RSG-I-UCS-18, was installed on the inside surface of the SCV model. As indicated in Figure 3.2, the pretest predictions of hoop strains at

this location show a significant discrepancy from the measured data at pressure levels above 2 MPa. The test data indicate that the local yielding started at 2.35 MPa, but the pretest prediction was for yielding to initiate at 3.2 MPa. In addition, at pressures above 3.2 MPa, the test data and the pretest predictions of hoop strains stay parallel and do not converge. The slopes of both curves decrease significantly at about 4 MPa, indicating that local contact between the SCV model and the contact structure might occur at this pressure.

This discrepancy between the predicted and measured yield pressures was consistent in most of the gage locations throughout the free-field areas of the SCV model. Figure 3.3 shows the external hoop strains at several gage locations in the upper conical shell section. As indicated in this figure, the pressure required to initiate general yielding of the SCV model was overestimated by about 30 percent and, furthermore, the post-yield deformations (or hoop strains) of the SCV model were consistently larger than those predicted by roughly the same percentage.

3.2 Posttest Analyses

The overall geometry of the SCV model is simple, and the finite element formulation should be capable of capturing the expected global behavior, but the discrepancies in the free-field behavior between the pretest predictions and the measured data were observed. The most probable cause for these comparison findings is the differences between assumed and actual material properties. The possible explanations for the mismatch between the assumed material properties and those more representative of the SCV model behavior have been addressed in Section 2.1.1.

The global three-dimensional finite element model of the SCV model and the contact structure for the posttest analysis effort has been discussed in Section 2.1.2 and is shown in Fig. 2.3. The nominal gap between the SCV model and the contact structure was increased from the nominal 18 mm to 22 mm to better reflect the as-built configuration. The enlarged gap size allowed larger deflections at some locations simply because there was more room for the SCV model wall to deflect outward. The changes to the material models in the posttest analysis in the lower strain regions and the increased gap size brought the

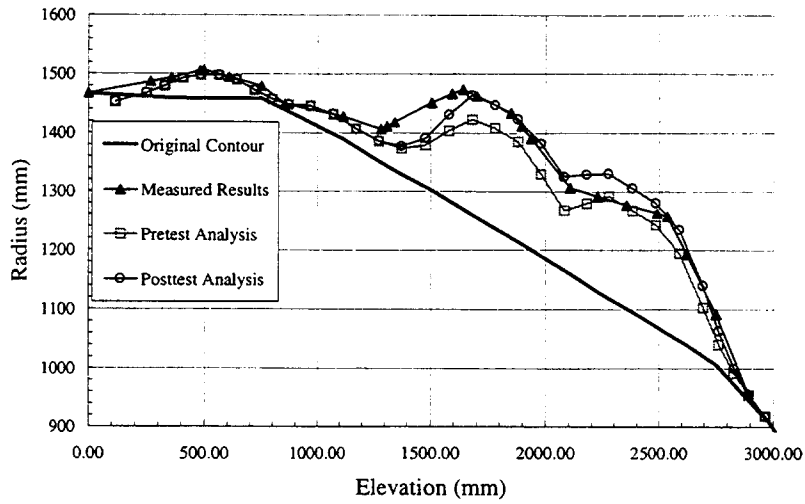


Figure 3.1 Radial deflections of the steel containment vessel (SCV) model (magnified by a factor of ten) at 4.5 MPa versus model elevation

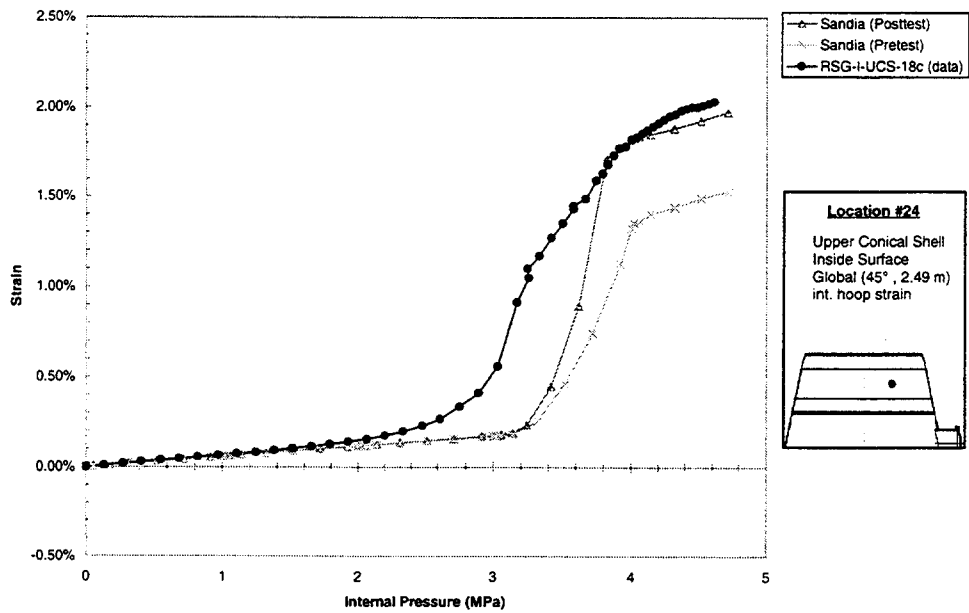


Figure 3.2 Interior hoop strains at upper conical shell section at Round Robin Standard Output Location #24

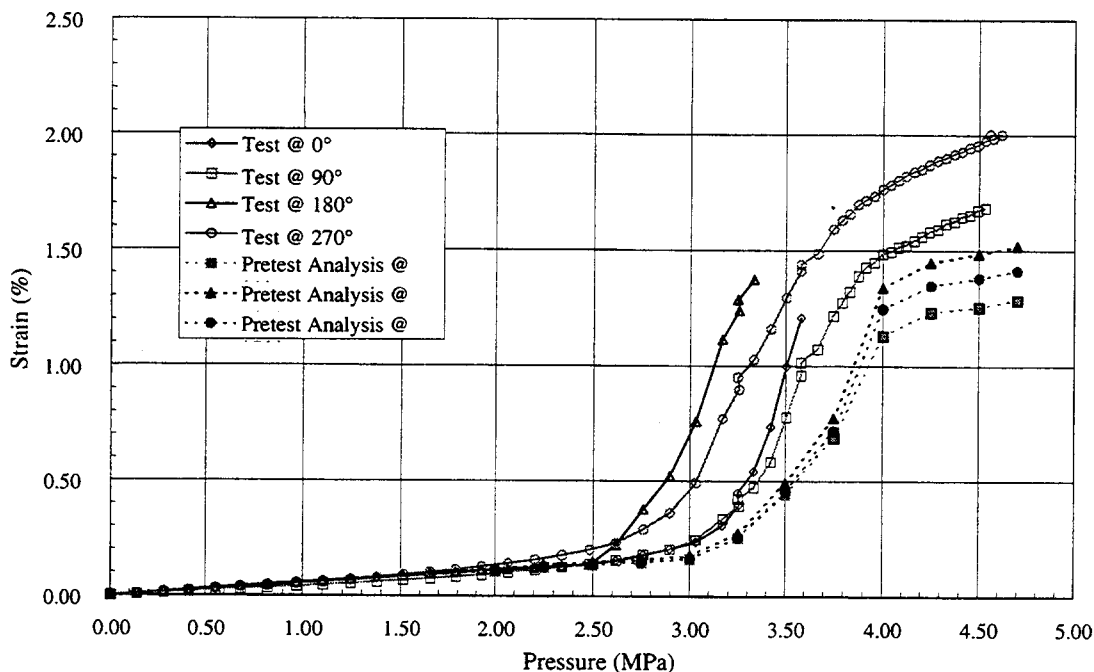


Figure 3.3 Exterior hoop strains at upper conical shell section

posttest analysis deflected shape much closer to the measured deflected shape, as demonstrated in Figure 3.1.

The effect of the increase in the gap between the SCV model and the contact structure on the global free-field behavior is also shown in Fig. 3.2. The posttest analysis results of hoop strains at the Round Robin Standard Output Location #24 eventually merged to the same value as the measured strains at a strain of about 1.75 percent. The pretest analysis results show the contact occurring at a much lower strain than the measured data. The increase in the gap to 22 mm in the posttest analysis represented the average as-built gap in the SCV model and led to results that matched the measured data well.

The hoop strains at the 270° meridian at 4.5 MPa plotted against the elevation of the SCV model are shown in Figure 3.4. The posttest analysis results, in comparison to the pretest predictions, demonstrate a much better correlation with the measured strains.

The major difference between the modeling procedures for the pretest and the posttest analyses with regard to the global behavior of the SCV model is the more accurate modeling of the material properties and a gap that is more representative of the as-built configuration. The test data indicate that the free-field hoop strains did not exceed 2 percent, which is only a small fraction of the ultimate strain for the steel materials. Therefore, attention to the low-strain behavior of each material is critical for an accurate prediction of the global behavior of the SCV model.

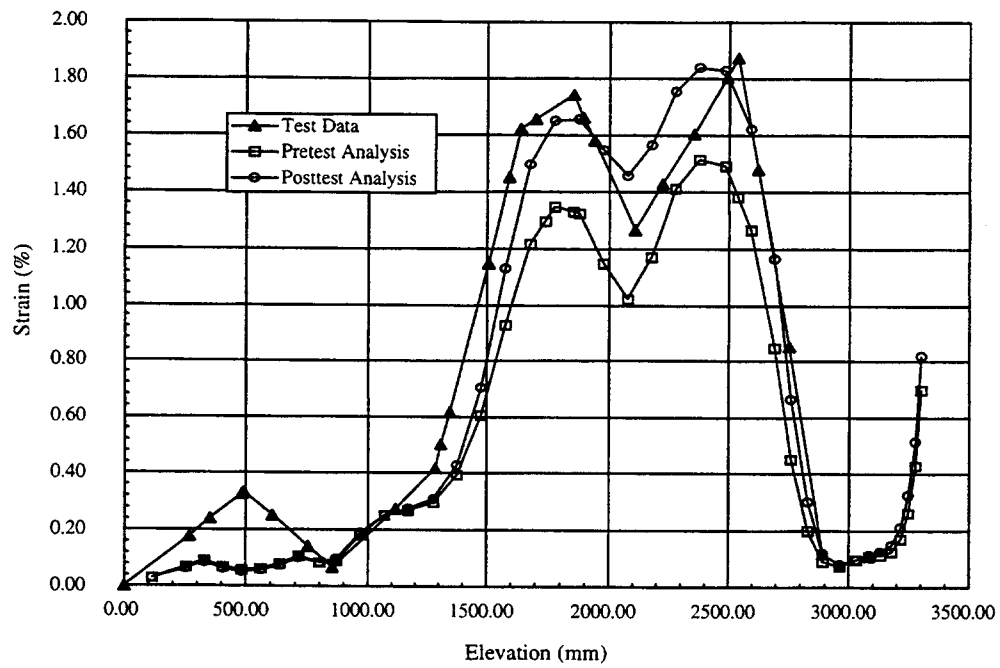


Figure 3.4 Hoop strains at 270° meridian and 4.5 MPa versus the steel containment vessel (SCV) model elevation

4. LOCAL ANALYSES

The posttest inspection of the steel containment vessel (SCV) model revealed that two tears developed in the SCV model during the high pressure test (Luk et al., 1999). A large tear, about 190 mm long, was found along the weld seam at the outside edge of equipment hatch reinforcement plate, and a small tear, approximately 55 mm long, inside a semi-circular weld relief opening at the middle stiffening ring. The pretest analysis results did not predict the occurrence of these two tears. The posttest metallurgical evaluation discovered that the large tear developed in a weakened heat affected zone (HAZ) in the SPV490 alloy (Van Den Avyle and Eckelmeyer, 1999) and the change in material strength caused by welding processes was not known prior to the high pressure test. The pretest analysis models did not simulate the structural details around the small tear; therefore no local strain concentration was predicted in its vicinity.

The posttest local analyses focused on developing the appropriate finite element models to calculate the local high-strain concentrations leading to the development of the two tears. An approximate material model with reduced strengths for SPV 490 HAZ was developed and incorporated in the local model for the large tear. A local model for the small tear was also developed to include the structural and geometric details around its neighborhood. This chapter discusses these local models and the analysis results.

4.1 Strength Reduction for SPV490 Heat Affected Zone

The material properties of both SGV480 and SPV490 alloys experienced changes when they were welded to fabricate the SCV model. The SGV480 material, which is mild steel, is not significantly affected with respect to its mechanical properties by the welding process. The posttest metallurgical evaluation of the SGV480 heat affected zone (HAZ) showed that the ultimate strength of the material essentially remained unchanged by the welding process (Van Den Avyle and Eckelmeyer, 1999). The HAZ is the parent material immediately next to the weld zone that is exposed to high temperatures during the welding process. The weld zone, consisting of the weld material with high yield strength, is not part of the HAZ.

The SPV490 alloy is a nominally higher-strength material that undergoes heat treatment during its

manufacture. The posttest metallurgical evaluation (Van Den Avyle and Eckelmeyer, 1999) found that the HAZ for this material in the SCV model did experience a significant reduction in strength (Van Den Avyle and Eckelmeyer, 1999). The heat from the welding process caused a localized microstructural alteration and resulted in a reduction of hardness and strength of SPV490 steel that is a martensitic/bainitic alloy (Van Den Avyle and Eckelmeyer, 1999).

The posttest metallurgical evaluation measured the Rockwell B hardness numbers for the base metal and the HAZ of SPV490 material. Lower hardness measurements were found in the HAZ than the base metal, indicating a reduction in material strength of the HAZ. It is very difficult to develop an accurate material model for SPV490 HAZ in the pretest state because such material is not available. Even if this material could be reproduced, the HAZ, in the shape of a very narrow strip, does not permit coupons to be machined for the standard tensile tests.

A simple method based on the relationship between strength and hardness numbers was then developed to determine the approximate material properties for SPV490 HAZ in the pretest state by using the SPV490 virgin material properties and the posttest hardness numbers for the HAZ and the base metal. A comprehensive set of tensile test data on virgin SPV490 steel plate was obtained prior to the high pressure test, but no hardness measurements were performed on the specimens. To obtain a set of material data having stress-strain relationship and hardness numbers from the same material, uniaxial tensile tests were performed on three coupons machined from the SPV490 steel plate used in the construction of the SCV model. All three tensile tests produced virtually identical stress-strain relationships. The calculated true stress versus true strain curve for one of the tests is plotted in Figure 4.1. The Rockwell B hardness numbers were also measured on the specimens machined from the same plate and were reported in the posttest metallurgical evaluation (Van Den Avyle and Eckelmeyer, 1999).

The approximate material properties for SPV490 HAZ in the pretest state were calculated according to the following procedure. First, the hardness number for the virgin plate together with the posttest hardness numbers for the HAZ and the local base metal were

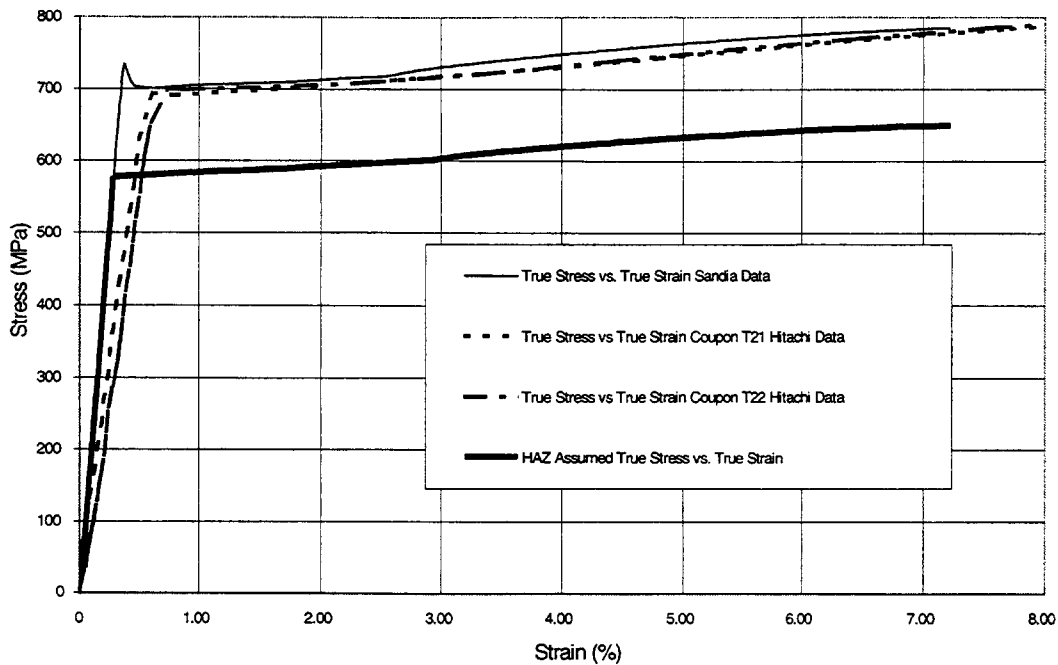


Figure 4.1 True stress versus true strain relationship for 9 mm SPV490 base metal and heat affected zone (HAZ)

used to calculate the approximate hardness number for the HAZ in the pretest state by using

$$H4 = H1 \times (H3/H2)$$

where

H1 = hardness number of the HAZ after the high pressure test = 91.21

H2 = hardness number of local base metal after the high pressure test = 97.4

H3 = hardness of the virgin plate material = 98.8
H4 = approximate hardness number of the HAZ in the pretest state

Therefore, the approximate hardness number for SPV490 HAZ in the pretest state is

$$H4 = 91.21 \times (98.8/97.4) = 92.52$$

Second, the hardness numbers were used to calculate the ultimate tensile strength based on an established correlation between these two properties of steels in accordance with the *ASM Metals Handbook* (1967).

The functional relationship between these two properties is shown in Figure 4.2. Accordingly, the ultimate tensile strength of the SPV490 HAZ in the pretest state (with hardness number of 92.52) is calculated to be 651 MPa (94.4 ksi), and that of the virgin plate (with hardness number of 98.8) is computed to be 784 MPa (113.7 ksi). Therefore, the ratio of reduction in ultimate strength between SPV490 HAZ and base metal is $651/784 = 0.83$. This procedure assumes that the fabrication process did not significantly change the hardness of the SPV490 material used in the SCV model.

Because there is not a well-defined relationship between the yield strength of steels and their hardness numbers, the same ratio of strength reduction is applied to the yield strength to approximate the entire curve of the post yield stress-strain behavior of SPV490 HAZ in the pretest state. The approximate yield strength obtained with this assumption is probably higher than the actual one because there is a smaller amount of strain hardening at the yield limit than at the ultimate strength level, but it is impossible to quantify this uncertainty due to lack of material data. This reduced strength material model, also plotted in Figure 4.1, was used to represent the

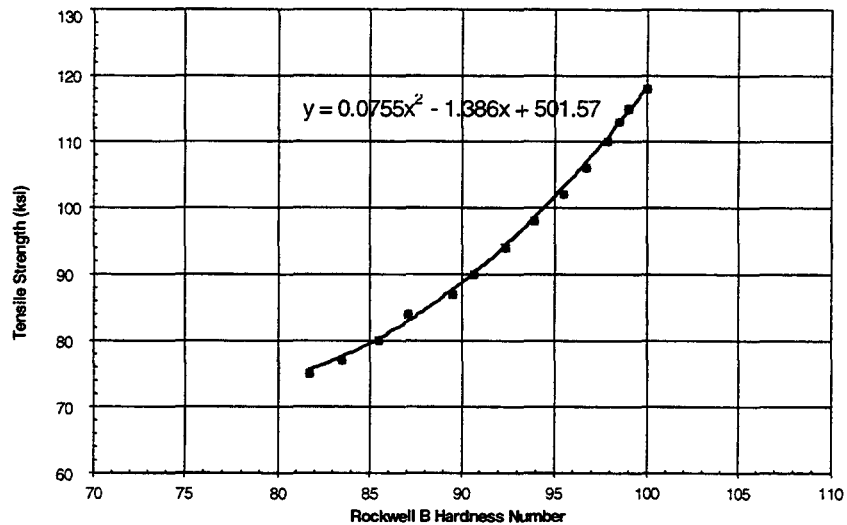


Figure 4.2 Correlation of Rockwell B hardness number to ultimate strength of SPV490 steel

SPV490 HAZ along the edge of equipment hatch reinforcement plate in the posttest analysis.

4.2 Equipment Hatch Analysis

Most of the complexity of the SCV model occurs in the equipment hatch area. In addition to the detail of the barrel-shaped equipment hatch, there is the added complexity of the thickened reinforcement plate around the penetration and a material change interface between SGV480 and SPV490 steels just below the horizontal centerline of the equipment hatch.

Other manufacturing details such as the eccentricities between the plates of different thicknesses make the equipment hatch area even more complex. Therefore, the equipment hatch area was heavily instrumented both inside and outside of the SCV model. Figure 4.3 shows the network of instrumentation on the interior of the SCV model. The large tear and the local thinned area on the other side of the equipment hatch detected posttest are also shown in the figure. Figure 4.4 is a schematic of the same area on the interior of the SCV model, showing the large tear, the thinned area and a few strain gages that recorded high strain readings.

A close-up photo of the large tear at the equipment hatch reinforcement plate is shown in Figure 4.5. The large tear in the model occurred at the lower left quadrant (looking from the inside of the SCV model) of the equipment hatch in the HAZ of the weld between the reinforcement plate and the 9 mm SPV490

plate. This is not the failure location predicted in the pretest analyses (Porter et al., 1998).

The pretest analyses predicted that a tear would occur in the 9 mm thick SPV490 material just below the material change interface just outside of the thickened reinforcement plate in a locally thinned area that was ground during the fabrication process. The actual failure occurred below this location in an area that would experience a relatively low strain deformation according to the pretest analysis prediction. Figure 4.6 shows the strain contours near the equipment hatch predicted by the pretest equipment hatch model without the locally thinned area. As indicated in this figure, the highest strains occur in the SGV480 material just above the material change interface.

The reason for the occurrence of the large tear at the SPV490 HAZ along the weld seam of the equipment hatch reinforcement plate has been explained in Section 4.1. The reduction in strength in the SPV490 HAZ material was not known prior to the high pressure test, so there were no pretest analyses addressing this situation. Although the pretest analysis report (Porter et al., 1998) mentioned the possibility of the failure being influenced by the HAZ material, there was no reason to believe before the test that the HAZ material would have a reduced strength.

When the approximate material model for SPV490 HAZ with a reduced strength, calculated in Section 4.1, is included in the local equipment hatch model in the posttest analysis, the area of highest strains moves

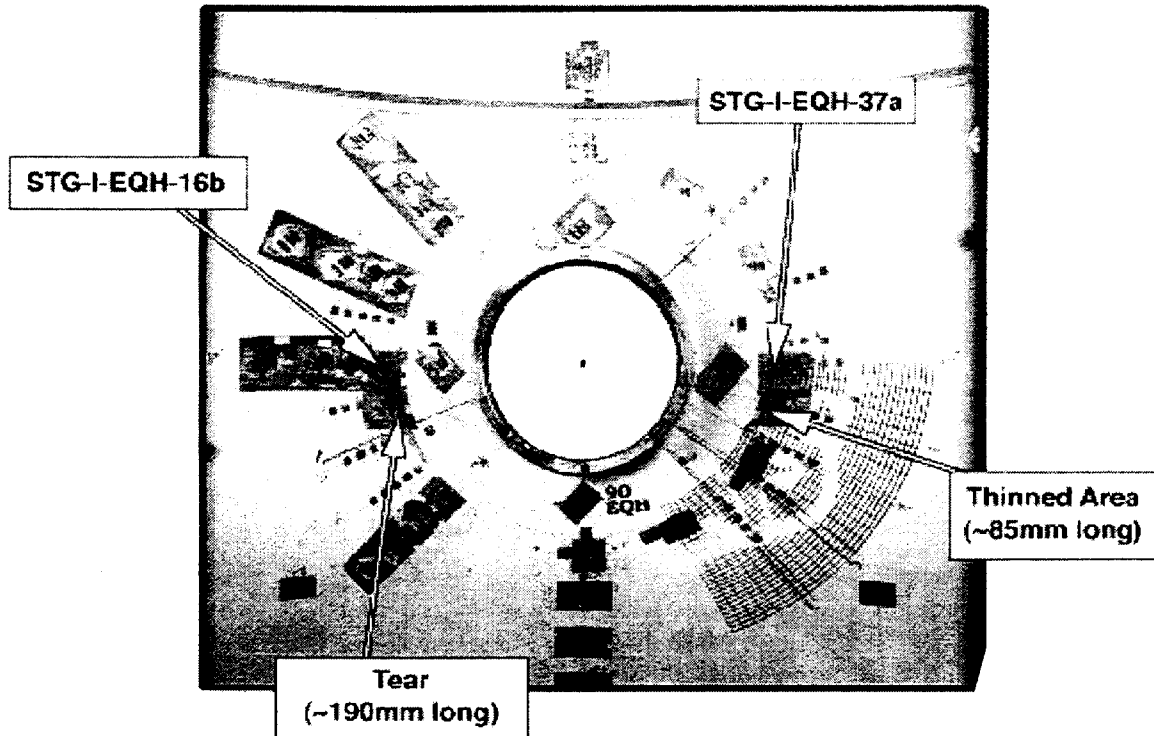


Figure 4.3 An instrumentation layout on the interior of the equipment hatch area

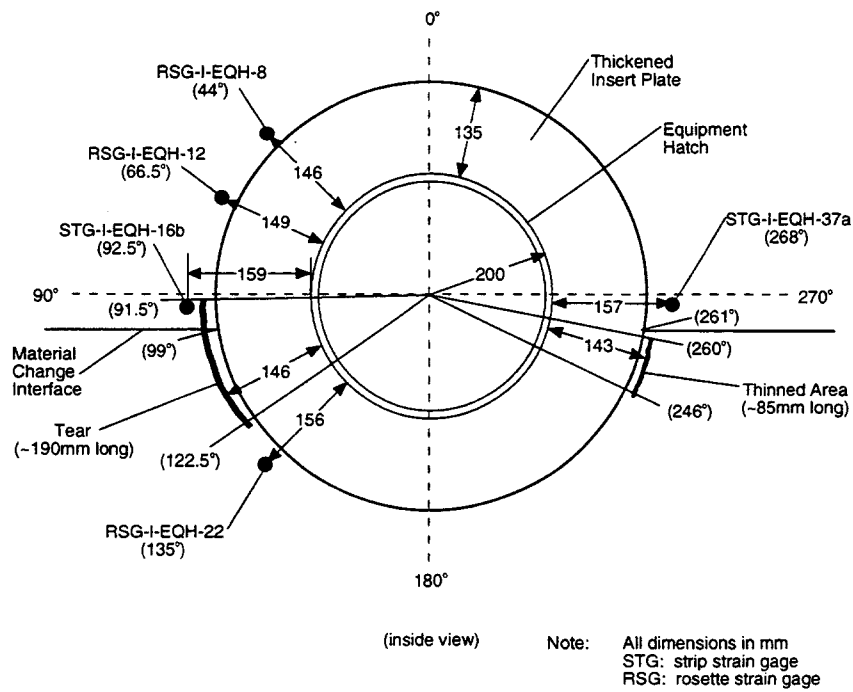


Figure 4.4 Schematic of the equipment hatch area from inside the SCV model



Figure 4.5 Interior view of equipment hatch area with an arrow pointing to large tear

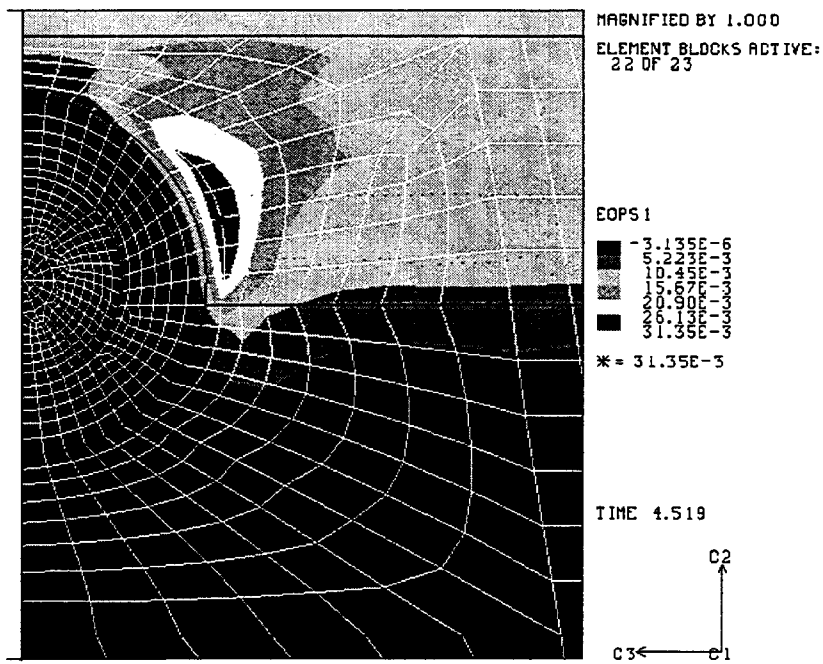


Figure 4.6 Strain contours around the equipment hatch from the pretest analysis

lower into the SPV490 material. The posttest simulations for the strain contours are shown in Figure 4.7.

As discussed in Section 4.1, the assumed yield strength in the approximate material model for SPV490 HAZ is probably higher than the actual one. It is very likely that SPV490 HAZ behaves like mild steel with a lower yield point. If this material approximation is used in the finite element analysis, even higher strains will be calculated around the area where the large tear developed during the test.

4.3 Middle Stiffening Ring Analysis

A small tear occurred in the SGV480 wall of the SCV model adjacent to a vertical weld inside a semi-circular weld relief opening at the middle stiffening ring. The small tear, with the local structural details, is shown in Figure 4.8. The posttest leak testing of the local area indicated that the tear went through the wall thickness. The other weld relief opening at the diametrically opposite location of the middle stiffening ring experienced local necking but did not fail. Because it is not likely that this small tear and the

large tear developed at the same time and pressure, the small tear must have formed at a lower pressure than the large tear and arrested itself as the pressure increased. The posttest analysis of the small tear focused on addressing the initiation and arrest mechanisms.

The middle stiffening ring is 61 mm wide and 19 mm thick. The radius of the semi-circular opening is 15 mm. This results in a reduction of about 25 percent in the cross sectional area of the ring. The posttest inspection of the SCV model revealed that the ring itself did not experience large strains as indicated by the intact paint on it near the opening, but the high strains occurred in the SGV480 wall adjacent to the vertical weld. A close-up of the local area of weld relief opening from the finite element mesh of the analysis model is shown in Figure 4.9. A large portion of the SGV480 wall was modeled to insure that the stress conditions in the local wall section near the stiffening ring were correct. The model was developed with the JAS3D finite element code (Blanford, 1998) using four-noded reduced-integration shell elements. The weld itself was not modeled in this analysis, and so there is no hardened or thickened area at the vertical centerline of the opening.

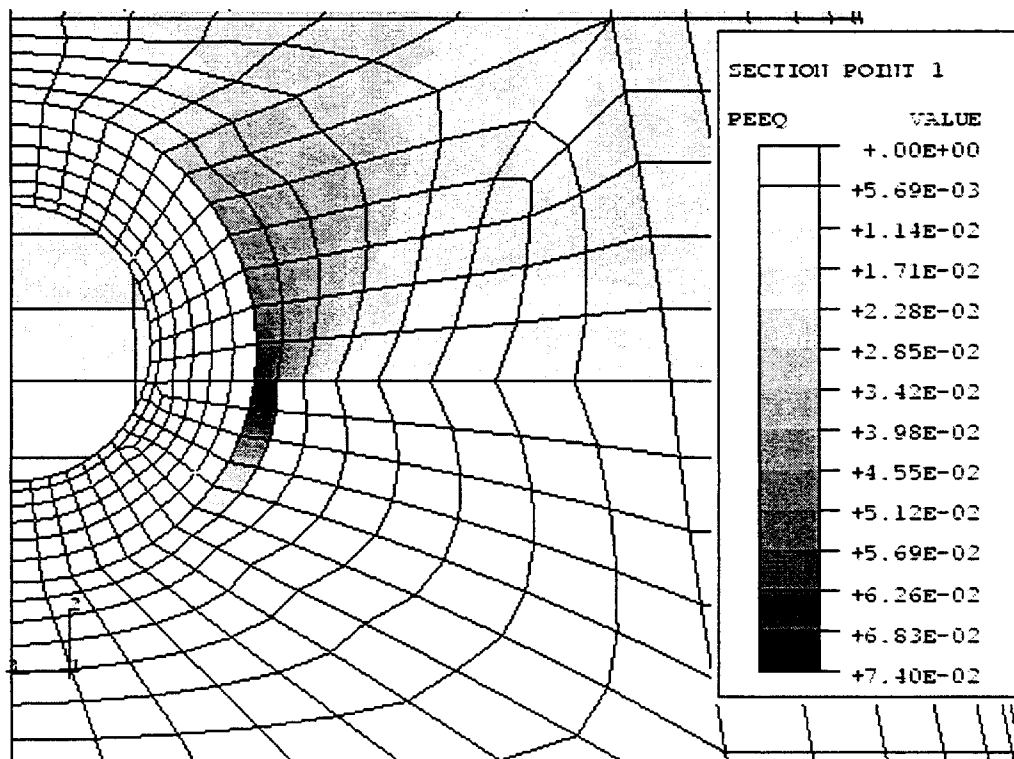
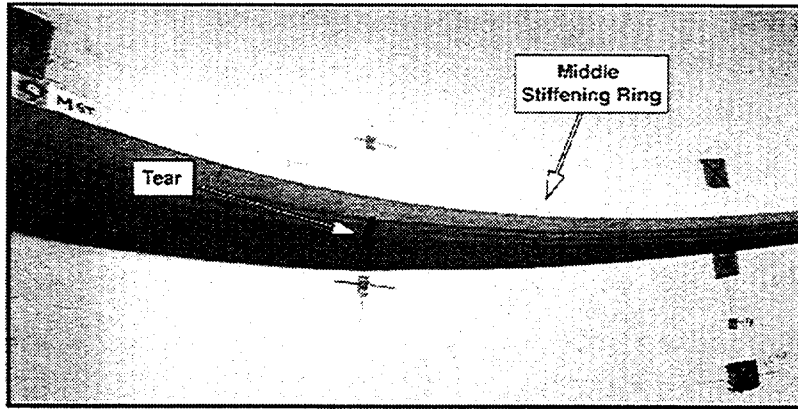
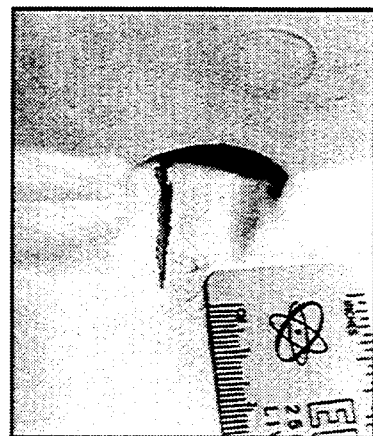


Figure 4.7 Strain contours around the equipment hatch from the posttest analysis



Above



Below

Figure 4.8 A small tear inside a weld relief opening at the middle stiffening ring

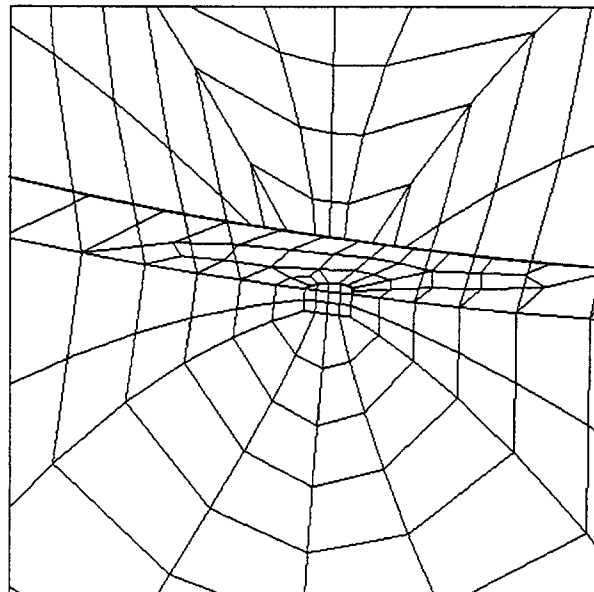


Figure 4.9 Close-up view of the weld relief opening at the middle stiffening ring from a local three-dimensional finite element model

Figure 4.10 shows a contour plot of the equivalent plastic strains on the inside surface of the SCV model at a pressure of 4.7 MPa. As indicated in this figure, the peak strains are concentrated in two areas on either side of the vertical centerline of the opening where the vertical weld would be located. The area of high strains coincides well with the location of the small tear in the SCV model. The local concentration of high strains on the inside surface results from a combination of increased hoop strains and bending strains due to the flattening out of the model wall.

The peak strains of 10.75 percent shown in the figure are misleading because the contact structure was not included in the analysis model. The contact structure would have limited the radial displacements and the hoop strains. The weld relief opening, with its detailed structural and geometric features, became a very efficient strain concentrator.

A more interesting issue is related to the arrest mechanism of the small tear. Figures 4.11 and 4.12 address this issue. In Figure 4.11, the posttest analysis results of the radial displacements at the tear location are shown. With an average gap of 22 mm, the outward radial displacement would have been stopped well before the over 50 mm of displacement

that is indicated in the figure. Just above the stiffening ring where the strains are larger, the SCV wall would have made contact with the contact structure at a pressure around 4.0 MPa, based on the measured data from strain gages and the results of posttest analysis. Figure 4.12 shows that, at 4.0 MPa, the equivalent plastic strain on the inside surface of the SCV wall just above the stiffening ring is about 1 percent. The tear at this low level of strain was most likely to be arrested given the condition that it was not allowed to propagate in the presence of the contact structure. Without the contact structure, this tear probably would not have been arrested and most likely would have been the initiating point for the failure of the SCV model during the high pressure test.

4.4 Failure Considerations of Steel Containment Vessel Model

Two factors need to be considered when predicting the large deformation behavior and the failure of a complex steel structure such as the SCV model subjected to loads causing stresses well into the plastic domain. First, it is important to have an accurate representation of the steel material properties at the low-strain range (< 2 percent) because the majority of the

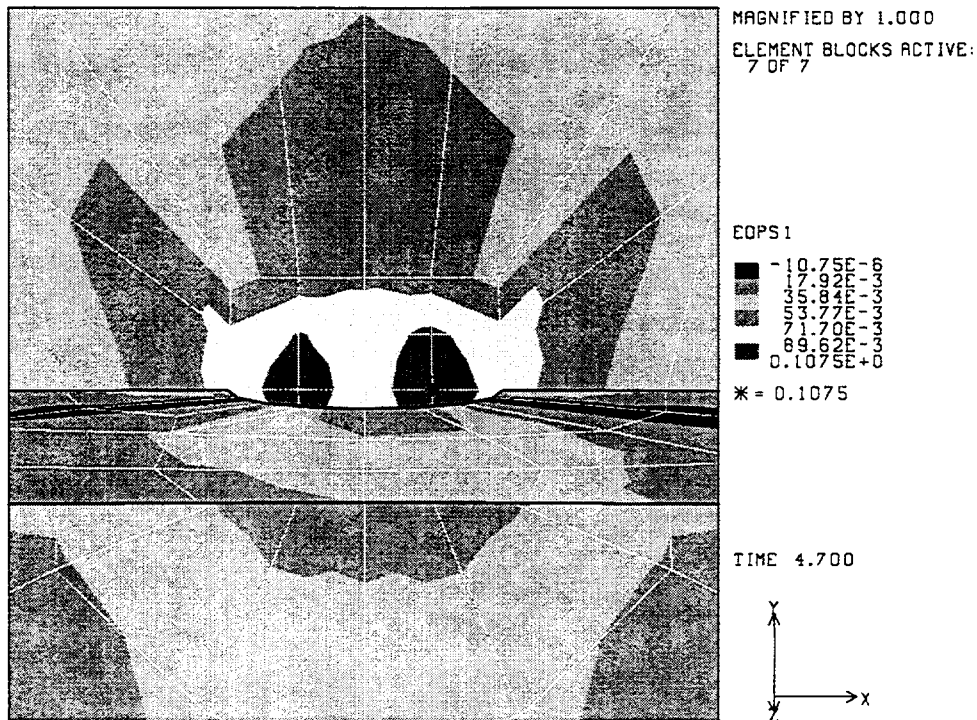


Figure 4.10 A contour plot of the equivalent plastic strains on the inside surface of the steel containment vessel (SCV) model at a pressure of 4.7 MPa

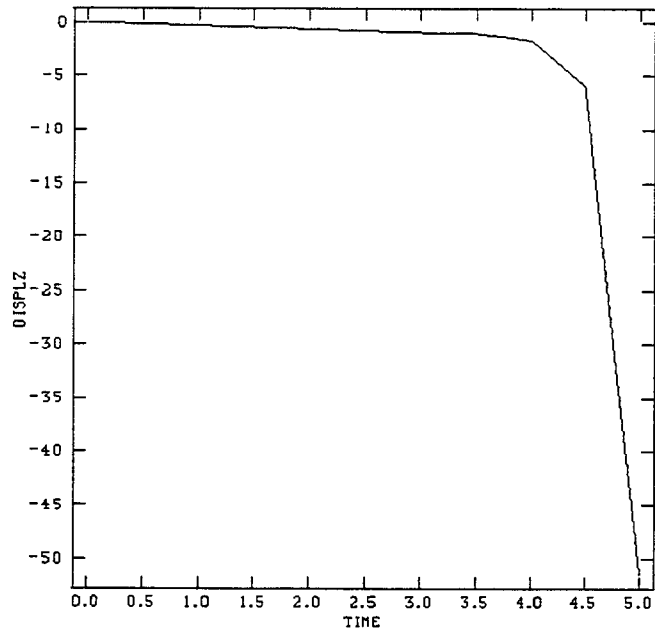


Figure 4.11 Outward radial displacement of steel containment vessel (SCV) wall at small tear location without the presence of contact structure

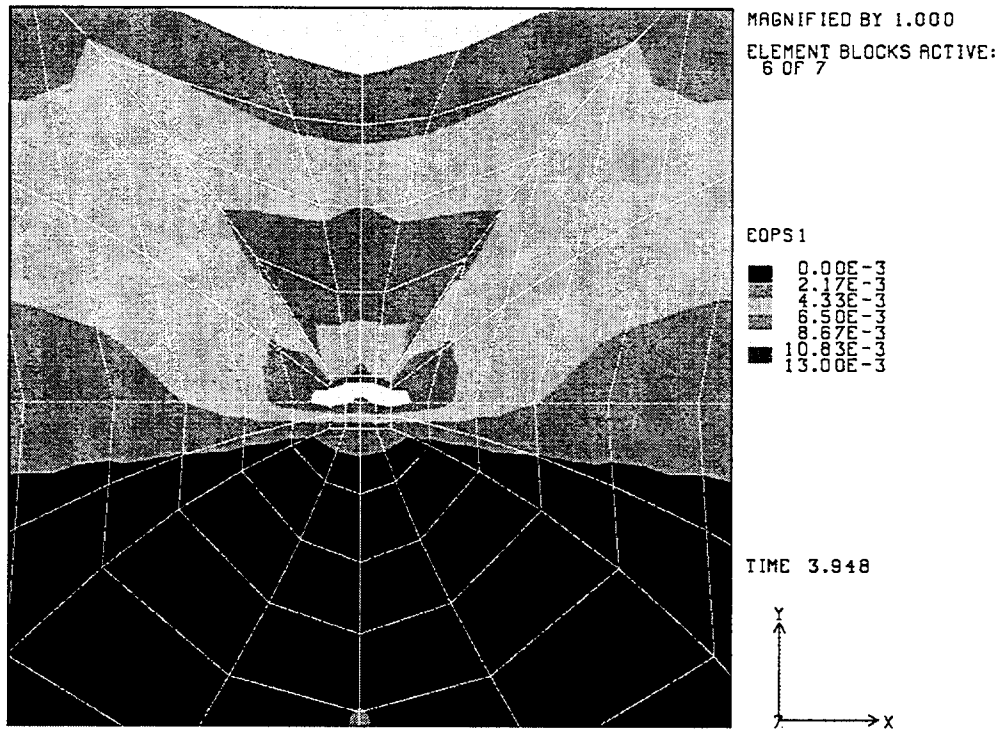


Figure 4.12 A contour plot of equivalent plastic strains on the steel containment vessel (SCV) wall adjacent to the weld relief opening at a pressure of 4.0 MPa

structural members experience strains in this range, even when a structural failure occurs due to a high-strain concentration at a local area. The global behavior at a free-field location is directly related to the steel material properties at the low-strain range. The deformation response of the structure is usually better comprehended in terms of its global behavior that is not affected by the local structural or geometrical details. The material models derived from the uniaxial tensile tests may not be representative of the material behavior in a large structure. The fabrication processes such as welding and shaping of structural members can significantly alter the material properties in the low-strain ranges.

Second, an accurate modeling of the local details is needed to predict the structural failure. Structures almost always fail in some local area where the detailed structural or geometric configurations cause high-strain concentrations to occur. In the pretest analyses, the criteria used to predict failure were assumed to be an equivalent plastic strain of 8 percent (Porter et al., 1998). The highest strain of 9 percent was recorded by a strain gage during the high pressure test in an area near the equipment hatch. The posttest analysis results showed a strain of 7 percent in the location where the large tear initiated. These findings are consistent with the pretest failure criteria. Therefore, for a ductile shear failure like the large tear in the SCV model, an equivalent plastic strain failure criterion seems appropriate.

5. SUMMARY

The comparison between the pretest analysis predictions and the measured data from the high pressure test identified three aspects of the analysis that needed to be addressed. First, an accurate material modeling of the stress-strain relationship, particularly in the low strain range, is required for improved simulations of the global response of the steel containment vessel (SCV) model. The pretest analysis used material models that were too stiff at low strains. Consequently, the pretest analysis results predicted the global response to yield at a higher pressure and to continue to deform at lower strain levels up to failure than what actually occurred during the test. The posttest analysis used the stress-strain relationships that represented the lower envelope of the uniaxial tensile material data. The revised material models in the posttest analysis did not include the effect of residual stresses, probably resulting in calculating yield pressures higher than those measured. The posttest analysis results of strains did in many cases converge toward the measured data as the strains increased.

Second, the posttest metallurgical evaluation revealed a weakened SPV490 HAZ along the weld seam at the edge of the equipment hatch reinforcement plate where the large tear developed during the test. When

welded, SPV490 steel alloy in the SCV model had a HAZ with reduced strength when compared to the parent material. The pretest analysis, using the SPV490 material model based on the uniaxial tensile data on parent material, predicted low strains around the location of the large tear. An approximate SPV490 HAZ material model with a reduced strength was developed and used in the posttest analysis models to calculate the high strain concentrations responsible for the initiation and propagation of the large tear.

Finally, the analysis models will not correctly predict the failure mode and mechanisms if the local structural and geometrical details that are responsible for the high-strain concentrations are not included in the analysis models. The SPV490 HAZ is a good example in this category. The other example is the presence of the semi-circular weld relief openings at the middle stiffening ring. The pretest analysis did not predict the high-strain concentrations around these openings because their details were not incorporated in the analysis models. After the local details of the openings were included in the posttest analysis models, the local strain concentrators leading to the development of the small tear inside the opening were identified.

6. REFERENCES

- ABAQUS: Standard User's Manual, Version 5.6.* 1995. Pawtucket, RI: Hibbitt, Karlsson, and Sorensen, Inc.
- ASM Metals Handbook, Desk Edition.* 1988. 2nd ed. Materials Park, Ohio: ASM International. 72–73.
- Blanford, M.L. 1998. JAS3D: "A Multi-Strategy Iterative Code for Solid Mechanics Analysis, User's Instructions, Release 1.4." Albuquerque, NM: Sandia National Laboratories.
- Luk, V.K., and Klamerus, E.W. 1998. *Round Robin Pretest Analysis of a Steel Containment Vessel Model and Contact Structure Assembly Subject to Static Internal Pressurization.* NUREG/CR-2899, SAND96-2899. Albuquerque, NM: Sandia National Laboratories.
- Luk, V.K., and Klamerus, E.W. 1999. *Round Robin Posttest Analyses of a Steel Containment Vessel Model.* NUREG/CR-5678, SAND98-2700. Albuquerque, NM: Sandia National Laboratories.
- Luk, V.K., Hessheimer, M.F., Rightley, G.S., Lambert, L.D., and Klamerus, E.W. 1999. *Design, Instrumentation, and Testing of a Steel Containment Vessel Model.* NUREG/CR-5679, SAND98-2701. Albuquerque, NM: Sandia National Laboratories.
- Pfeiffer, P.A., and Kulak, R.F. 1988. "Residual Stress Effects in Containment Analysis," S.J. Chang, and D. Brochard, eds. Published in *Technologies in Reactor Safety, Fluid-Structure Interaction, Sloshing and Natural Hazards Engineering.* ASME Publication PVP, Vol. 366. 21–30.
- Porter, V.L., Carter, P.A., and Key, S.W. 1998. *Pretest Analysis of the Steel Containment Vessel Model.* NUREG/CR-6516, SAND96-2877. Albuquerque, NM: Sandia National Laboratories.
- Van Den Avyle, J.A., and Eckelmeyer, K.H. 1999. *Posttest Metallurgical Evaluation Results for the Steel Containment Vessel (SCV) High Pressure Test.* SAND98-2702. Albuquerque, NM: Sandia National Laboratories.

NRC FORM 335 (2-89) NRCM 1102, 3201, 3202	U.S. NUCLEAR REGULATORY COMMISSION BIBLIOGRAPHIC DATA SHEET <i>(See instructions on the reverse)</i>	1. REPORT NUMBER (Assigned by NRC, Add Vol., Supp. Rev., and Addendum Numbers, if any) NUREG/CR-6649 SAND99-2954
2. TITLE AND SUBTITLE Posttest Analysis of the Steel Containment Vessel Model	3. DATE REPORT PUBLISHED	
	MONTH February	YEAR 2000
	4. FIN OR GRANT NUMBER A1401	
5. AUTHOR(S) John S. Ludwigsen/Sandia National Laboratories Vincent K. Luk/Sandia National Laboratories Michael F. Hessheimer/Sandia National Laboratories	6. TYPE OF REPORT Technical	
	7. PERIOD COVERED <i>(inclusive Dates)</i> 5/97 to 2/99	
8. PERFORMING ORGANIZATION – NAME AND ADDRESS <i>(If NRC, provide Division, Office or Region, U.S. Nuclear Regulatory Commission, and mailing address; if contractor, provide name and mailing address.)</i> Sandia National Laboratories P. O. Box 5800, MS 0744 Albuquerque, NM 87185-0744		
9. SPONSORING ORGANIZATION – NAME AND ADDRESS <i>(If NRC, type "Same as above", if contractor, provide NRC Division, Office or Region, U.S. Nuclear Regulatory Commission, and mailing address.)</i> Division of Engineering Technology Office of Nuclear Regulatory Research U.S. Nuclear Regulatory Commission Washington, D.C. 20555		
10. SUPPLEMENTARY NOTES J.F. Costello, NRC Project Manager		
11. ABSTRACT <i>(200 words or less)</i> The Nuclear Power Engineering Corporation (NUPEC) of Japan and the U.S. Nuclear Regulatory Commission (NRC) are co-sponsoring and jointly funding a Cooperative Containment Research Project at Sandia National Laboratories (SNL) to conduct a high pressure test of a steel containment vessel (SCV) model and contact structure assembly on December 12-13, 1996. The project objectives are to provide data of the structural response of the model up to its failure in order to validate analytical modeling, to find its pressure capacity, and to observe the failure mode and mechanisms. The SCV model is a mixed-scale model (1:10 in geometry and 1:4 in shell thickness) of a steel containment for an improved Mark-II Boiling Water Reactor (BWR) plant in Japan. A pretest analysis of the SCV model (NUREG/CR-6516) was performed to predict the model response to loads beyond the design basis conditions. The posttest analysis effort compared the pretest analysis results to the high pressure test data and identified the areas of discrepancies. The posttest analyses were then undertaken to investigate if the more accurate material models and the local structural and material details around the two tears in the SCV model developed during the high pressure test could improve the analytical predictions. This report documents the posttest analysis results and summarizes the lesson learned from the analysis effort.		
12. KEY WORDS/DESCRIPTORS <i>(List words or phrases that will assist researchers in locating the report.)</i> <i>Finite Element Analysis, Reactor Containments, Steel Containment Vessel, Severe Accidents, Structural Response, Pretest Prediction, Posttest Simulation, Failure Pressure and Mechanisms.</i>	13. AVAILABILITY STATEMENT Unlimited	
	14. SECURITY CLASSIFICATION <i>(This Page)</i> Unclassified	
	<i>(This Report)</i> ... Unclassified	
	15. NUMBER OF PAGES	
16. PRICE		



Federal Recycling Program